



ELSEVIER

Journal of Nuclear Materials 297 (2001) 113–119

Journal of
nuclear
materials

www.elsevier.com/locate/jnucmat

Investigation on the oxidation characteristics of copper-added modified Zircaloy-4 alloys in pressurized water at 360°C

Hyun Seon Hong^{*}, Jae Sik Moon, Seon Jin Kim, Kyung Sub Lee

Department of Materials Science and Engineering, Hanyang University, Seoul 133-791, Republic of Korea

Received 9 March 2001; accepted 28 April 2001

Abstract

In order to assess the influence of copper addition on the oxidation behavior of modified Zircaloy-4 (Zry-4) alloys as well as Zr–Cu binary alloys, weight gain changes in a pressurized autoclave at 360°C were investigated. The copper content varied from 0.1 to 0.8 wt% for the binary alloys and changed from 0 to 0.5 wt% for the modified Zry-4 alloys. The optimum copper content for improved oxidation resistance turned out to be in the range 0.1–0.2 wt% from weight gain measurements; in the binary alloy, the weight gain generally decreased with decreasing Cu content from 0.8 to 0.2 wt% although 0.1 wt% Cu specimen showed higher weight gain than 0.2 wt% Cu specimen. This tendency was observed in the modified Zry-4 alloy showing the lowest weight gain at 0.1 wt% Cu content. To understand the microstructural influence on oxidation of the copper-added zirconium alloys, the effects of copper additions on the crystal structure of the oxide, second phase precipitates and microstructure of the metal matrix were studied. © 2001 Elsevier Science B.V. All rights reserved.

1. Introduction

The recent trend towards extended burn-up with high coolant lithium levels in PWR has led to an increased demand on the oxidation resistance of cladding materials. The development of advanced cladding is relevant to safety because improved oxidation resistance will reduce the number of cladding failures during anticipated transients and during LOCAs. Many efforts have been devoted to modify or optimize the Zry [1,2] as well as to develop other alloy systems [3,4]. The authors have participated in that research for some years and already have published some results on mechanical properties of copper-added modified Zry-4 alloys [5]. The paper was related to a very specific point of view, namely to the increase of strength of Zry-4 by alloying with copper as a potential substitute of tin. The present study is part of

the authors' continuing research in finding the optimum copper content for improving the mechanical and oxidation properties of cladding materials. In this study, the effects of copper addition on oxidation properties are investigated.

Steam or water autoclave oxidation tests have been used over the years to simulate the waterside oxidation of Zry. Weight gain is usually investigated as a measure of oxidation resistance in autoclave tests. This method may determine the oxidation behavior of specific zirconium alloys or may differentiate between the different alloys within specific conditions such as temperatures, pressures and so on. However, this technique, measuring weight gain, cannot predict the oxidation behavior correctly outside these conditions. Some approaches have been attempted to solve this problem by presenting an oxidation model based on the material microstructure that it may explain the PWR oxidation behavior of Zry-4 but no explicit study has yet to be performed [6,7]. The objective of the present study is to assess the influence of copper addition on oxidation behavior of the modified Zry-4. Autoclave oxidation tests in pure water at 360°C were conducted up to 100 days and weight gain changes were observed as a

^{*} Corresponding author. Present address: Department of Nuclear Engineering, University of California at Berkeley, 4164 Etcheverry Hall, Berkeley, CA 94720, USA. Tel.: +1-510 642 7158; fax: +1-510 643 9865.

E-mail address: hshong@nuc.berkeley.edu (H.S. Hong).

measure of oxidation resistance. In addition, in order to evaluate the effect of copper addition on the oxidation behavior, the microstructural parameters such as oxide structure, precipitate distribution, and grain structure were characterized with increasing copper content.

2. Experimental procedures

2.1. Specimen preparation

Three classes of copper-added zirconium alloys were prepared as follows. In the first class, specimens have the standard tin content of Zry-4 (1.5 wt%). The Fe/Cr ratio of Zry-4 was reduced to 0.5 and the copper content varied from 0 to 0.5 wt%. In the second class, the tin content was reduced to 1.0 wt% and the Fe/Cr ratio was maintained at 0.5. In addition, the copper content was increased up to 0.5 wt%. In the third class, Zr–Cu binary specimens were prepared by changing the copper content from 0.1 to 0.8 wt%. The chemical compositions of the present specimens are listed in Table 1.

The specimens were prepared according to the following procedures. Pure reactor grade sheet-type Zr and alloying elements were arc melted into 100 g button type ingots. Homogenized ingots were β forged at 1010°C and quenched into water. After the β quenching, the ingots were hot-rolled at 700°C and annealed at 650°C under an argon atmosphere. The plates were then cold-rolled and annealed at 700°C for 1 h for recrystallization. The oxide scale formed on the plates during these thermomechanical treatments was removed by mechanical polishing and pickling in a mixed solution of 10% HF, 45% HNO₃ and 45% H₂O before the test specimens were machined to their final shape.

Table 1
Chemical composition (in wt%) of the Cu-added Zr alloys

Specimen number	Alloying elements				
	Sn	Fe	Cr	Cu	Zr
1	1.5	0.1	0.2	0.0	Balance
2	1.5	0.1	0.2	0.1	Balance
3	1.5	0.1	0.2	0.5	Balance
4	1.0	0.1	0.2	0.05	Balance
5	1.0	0.1	0.2	0.1	Balance
6	1.0	0.1	0.2	0.2	Balance
7	0.0	0.0	0.0	0.1	Balance
8	0.0	0.0	0.0	0.2	Balance
9	0.0	0.0	0.0	0.3	Balance
10	0.0	0.0	0.0	0.5	Balance
11	0.0	0.0	0.0	0.8	Balance
12	Conventional Zircaloy-4				

2.2. Microstructural analysis of precipitates

Scanning electron microscopy (SEM) and scanning transmission electron microscopy (STEM) were performed to characterize the precipitates in the metal phase before the oxidation test. The crystal structure was determined by selected area electron diffraction (SAD) pattern, and quantitative analysis of precipitates was performed using STEM with energy dispersion spectroscopy (EDS). It is a useful instrument for analyzing chemical compositions of intermetallic precipitates smaller than 10 nm because the small size of beam probe (approximately 20 nm) permits excellent spatial resolution by centering the beam within the particle of interest. STEM samples were mechanically polished to 50 μ m and jet-polished in a solution of 90% ethanol and 10% perchloric acid at –40°C and 13 V. SEM samples were etched in a solution of 5% HF, 45% HNO₃ and 50% H₂O.

2.3. Oxidation tests

The specimens for oxidation tests were prepared by the procedures described in the previous study [1]. The oxidation tests were conducted in autoclaves filled with pure water at 360°C under a pressure of 180 bar. Oxidation test specimens with the dimension of 10 mm \times 25 mm \times 1 mm were prepared from the recrystallized sheet specimens. The specimens were mechanically and chemically polished before testing. The test followed the ASTM G2 method [8]. The oxidation behavior was evaluated by the weight gain (ΔW) as a function of exposure time.

2.4. Oxide analysis

In order to identify the crystal structure of the growing oxide surface Raman spectroscopy was used. The methods of characterization of the structure of ZrO₂ by a Raman spectrometer have been reported elsewhere [9–11]. A Raman spectrometer with a 200 mW argon-ion laser source at a wavelength of 488 nm was used. The spectral range employed was from 100 to 500 cm⁻¹.

Impedance measurements were carried out for oxide films on Zr–Cu alloys to examine the behavior of precipitates located in the oxide films. Samples were oxidized in pressurized water at 360°C for different times to form oxide films with equal thickness. The electrical resistivity of oxide films was measured under alternating current conditions using an electrochemical impedance measurement system. Samples were stabilized for 12 h in a solution of 1 M H₂SO₄ with a Pt counter electrode and a calomel reference electrode. The frequency range employed was from 10⁻³ to 5 \times 10³ Hz.

3. Results and discussion

3.1. Weight gain

Fig. 1(a) shows the weight gain vs. copper content curve for Zr–Cu binary alloys after 50 days exposure. It can be seen that small additions of copper around 0.2 wt% lowered the weight gain. However, further additions higher than 0.2 wt% or those less than 0.2 wt%

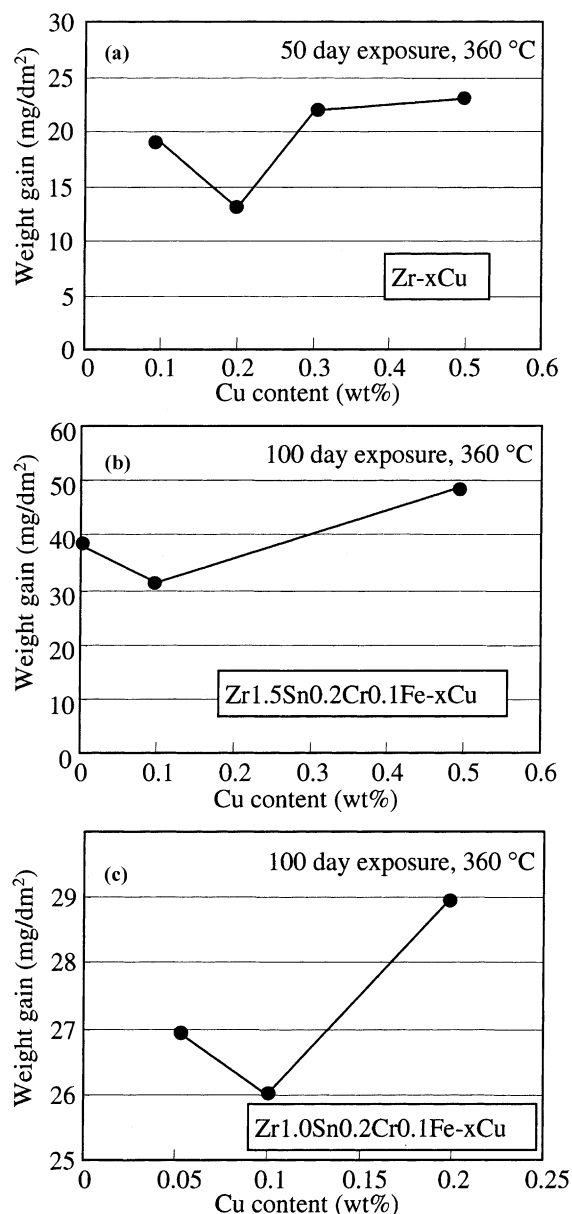


Fig. 1. The weight gain vs. copper content curve for: (a) Zr–Cu binary alloys, (b) Zr–1.5Sn–0.1Fe–0.2Cr–Cu alloys, (c) Zr–1.0Sn–0.1Fe–0.2Cr–Cu alloys.

increased the weight gain showing that 0.2 wt% is the optimum Cu content for improved oxidation resistance in the conditions of the test. The weight gain generally increased with increasing copper content in the range 0.2–0.5 wt%. The specimen with 0.8 wt% Cu showed the linear oxidation rate. The weight gain of this specimen reached hundreds of mg/dm² even after 10 days exposure and so this test was terminated in 10 days due to heavy oxidation.

The oxidation rate exponents (n) obtained from the log–log plots of $W^n = kt$ where W , k , t are weight gain, rate constant, and time, respectively, were in the range 2.3–3.4 indicating that the alloy followed the cubic rate law. It is probable that the oxidation of zirconium alloys does not obey the simple diffusion-controlled parabolic rate law but follows the cubic rate law [12,13]. The cubic rate laws were explained as a combination of diffusion-controlled oxide formation and oxygen dissolution into the metal in the previous studies. The parabolic rate was modified because the simple diffusion reaction of oxygen was complicated by oxygen dissolution into the zirconium matrix [1,2].

Fig. 1(b) represents the weight gain change with the copper content in the modified Zry-4 alloys after 100 days exposure. The oxidation rate exponents (n) were in the range 2.5–3.6 showing the cubic rate law. The oxidation kinetics of copper-containing zirconium alloys studied in this work was, therefore, thought to be similar to that of conventional Zry-4. As seen in the graph, the weight gain was reduced as the copper content decreased from 0.5 to 0.1 wt%. The weight gain of the copper free specimen was, however, higher than that of the 0.1 wt% copper specimen. The lowest weight gain was shown at 0.1 wt% copper content. In order to verify this optimum copper concentration for improved oxidation resistance in copper-added modified Zry-4 alloys, the characteristics of weight gain in other alloys, that is, the alloys having low Sn (1.0 wt%) content were investigated. The variation of weight gain with the copper content less than 0.2 wt% is shown in Fig. 1(c). When the copper content was lowered from 0.2 to 0.1 wt%, the weight gain decreased. However, if the copper content decreased further to 0.05 wt% then the weight gain increased. This result is consistent with the trend obtained from the specimens with 1.5 wt% Sn shown in Fig. 1(b). It is to be noted that this value is lower than that of conventional Zry-4; the weight gain of Zry-4 measured in the same autoclave testing condition was about 40 mg/dm². Conclusively, the small addition of copper less than 0.2 wt% could generally improve the oxidation resistance of copper-added zirconium alloys in the conditions of the tests. This tendency is also observed in the Zr–Nb system [14]. The oxidation resistance of zirconium-based alloys was improved by a small addition of Nb (about 0.05–0.2 wt%) compared with that of Zry-4. Many efforts have been devoted to design

niobium-containing zirconium alloys in order to develop an alloy with improved oxidation resistance and equivalent mechanical properties to Zry-4.

The oxidation rate is mainly associated with the following oxidation processes: the diffusion of oxygen ions, the electron migration, and the oxygen dissolution from the oxide/metal interface to the metal inside [15–18]. In this study, the change in oxide structure was investigated with respect to the diffusion of oxygen ions, precipitate distribution to the electron migration, and matrix grain structure to the oxygen dissolution.

3.2. Oxide structure

In the authors' previous study, the oxide of Zry-4 in the pre-transition region was found to be a mixture of tetragonal and monoclinic phase [1,2]. The amount of the tetragonal phase in the oxide, evaluated by laser Raman spectroscopy, was around 40% before the rate transition. This tetragonal phase is believed to be more protective against oxidation than the monoclinic phase. Thus, smaller amounts of the tetragonal phase in the oxide will cause faster oxygen diffusion, thereby increasing weight gain [19,20]. Fig. 2 shows the inverse relationship of weight gain change with fraction of the tetragonal phase in the present specimens. When the weight gain increased, the tetragonal fraction decreased as seen in the graph. It is to be noted that the points in this plots represent the weight gain obtained from the specimens with different composition.

It is well known that the amount of the tetragonal phase can be influenced by alloying elements. For example, Harada et al. [21] studied the oxide structure with changing tin content. In the specimen less than 0.1 wt% tin, the oxide consisted of monoclinic and tetragonal phases. However, in the specimen containing 2.2 wt%

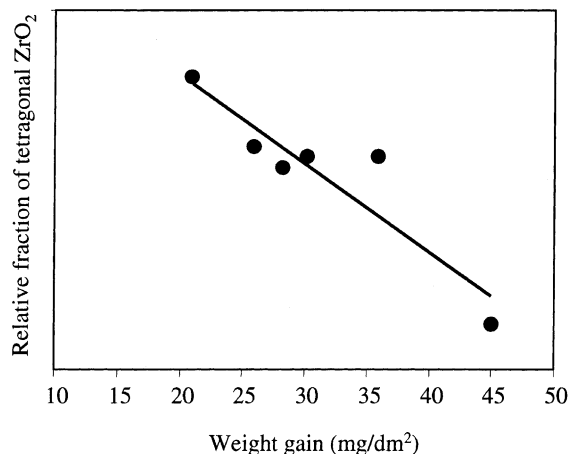


Fig. 2. Dependence of amounts of tetragonal phase on weight gain change.

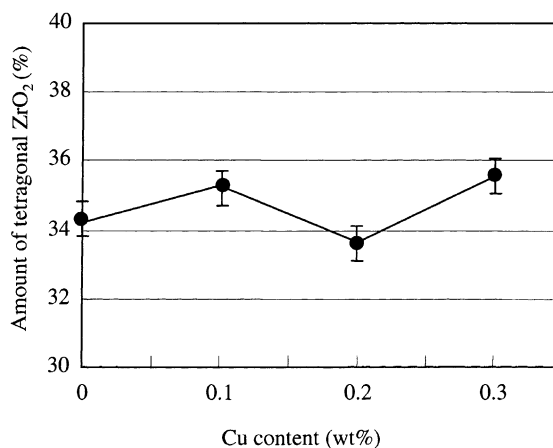


Fig. 3. Variation of tetragonal phase fraction in oxide of Zr-based alloys.

tin, only the monoclinic phase was observed. Thus, they suggest that tin stabilizes the monoclinic phase. In the present study, the oxide structures of the Zr–Cu binary specimens were investigated after 10 days exposure by Raman spectroscopy as shown in Fig. 3. The analysis showed that the oxide structure was a mixture of tetragonal and monoclinic phases and the amount of the tetragonal phase was about 35% regardless of the copper content. The copper addition does not seem to affect the initial amount of the tetragonal phase of the oxide (after 10 days exposure) under the present testing conditions.

3.3. Second phase precipitates

Electron migration through the oxide layer is related to the precipitate size distribution as follows. Under PWR conditions, as the precipitate size decreases down to the critical value of 0.1 μm , the oxidation resistance will decrease. The small precipitates can readily form a chain-like network in the oxide [22]. These fine chain-like precipitates act as a fast path of electron migration during the oxidation process. Thus, the small precipitates are believed to accelerate the electron migration and the subsequent oxidation reaction. In addition, if small precipitates are irradiated, they will be dissolved in the oxide and the oxidation reaction will be accelerated due to the increase in electron conduction [23].

The types of the present precipitate were identified. For the modified Zry-4 specimens, three main precipitates were found: namely, (1) $\text{Zr}(\text{Fe}, \text{Cr})_2$ precipitates in both copper-added and copper-free specimens; (2) $\text{Zr}(\text{Fe}, \text{Cr}, \text{Cu})_2$ precipitates, and (3) Zr_2Cu precipitates in the copper-added specimen. For Zr–Cu binary specimens, only one kind of Zr_2Cu precipitate was observed. The intermetallic phase $\text{Zr}(\text{Fe}, \text{Cr})_2$ is reported to have either the C-14 hexagonal or the C-15 cubic prototype

Laves phase structure [24–27]. In this study, the $Zr(Fe, Cr)_2$ precipitate was found to have C-14 type hexagonal structure, and STEM study showed that the relative proportion of Fe and Cr in the precipitate was close to its nominal value in the alloy. Quantitative analysis showed that the $Zr(Fe, Cr, Cu)_2$ precipitate was also identified to be the C-14 type hexagonal structure, however, the Zr_2Cu precipitate was found to be the tetragonal structure.

Sizes of $Zr(Fe, Cr)_2$ and $Zr(Fe, Cr, Cu)_2$ precipitates were measured to be around 0.1 μm and were always less than 0.3 μm . These precipitates were not as large as the largest Zr_2Cu precipitates. The size of Zr_2Cu precipitates ranged from 0.25 to 0.57 μm and the number of the precipitates was much smaller than that of $Zr(Fe, Cr)_2$ and $Zr(Fe, Cr, Cu)_2$ precipitates. The average size of the precipitates increased from 0.10 to 0.16 μm and the area fraction increased from 1.13% to 3.92% as the copper content increased from 0.1 to 0.5 wt% in the specimen with 1.5 wt% Sn (specimens # 1, 2 and 3). The specimens with 1.0 wt% Sn (specimens # 4, 5 and 6) showed similar results to that of the specimens with 1.5 wt% Sn as shown in Table 2. In general, a higher copper content shows larger precipitates and higher area fractions. It is considered that the roles of copper in the precipitates of the present specimens are to form a binary zirconium–copper precipitate or to replace Fe or Cr in the $Zr(Fe, Cr)_2$ precipitate, and thus to increase the size and the area fraction of precipitates.

In the present experiment, electrical resistivities of oxide films were measured from the specimens that had different copper contents using the impedance test. Fig. 4 shows the resistivity change with varying copper contents in Zr–Cu binary specimens. Data points for the resistivity in Fig. 4 were obtained from the frequencies of 7.92×10^{-3} and 1.99×10^{-3} Hz, which showed typical

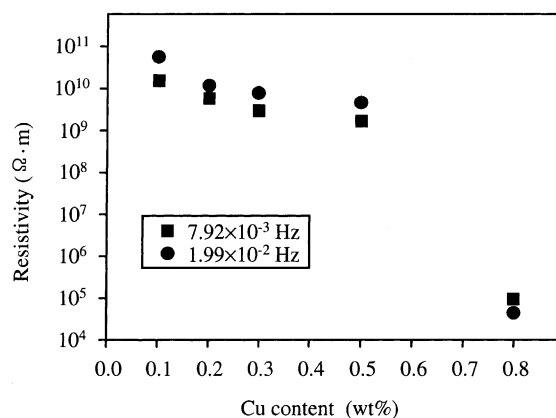


Fig. 4. Electrical resistivity of ZrO_2 oxide film on Zr–Cu alloys with varying Cu content.

resistivity results. The resistivity decreased as the copper content increased from 0.1 to 0.8 wt%. Apparently, the higher copper content specimen that has a large volume fraction of precipitates seems to provide more electron migration paths. Thus, the increase in copper content is thought to be responsible for the increase in electronic conduction and the acceleration of oxidation.

3.4. Grain structure

The β -zirconium phase has been reported to have a better oxidation resistance than the α -zirconium phase. In the β -quenched condition, the alloy contains a large fraction of low-soluble alloying elements in supersaturation. Supersaturation might be one of the reasons for the improved oxidation resistance. Some researchers investigated the effect of alloying elements, such as tin, titanium, carbon and oxygen, on the β -quenched microstructure and concluded that the structure is very sensitive to the alloying elements [28–30]. The phase diagram of the Zr–Cu system has been extensively studied [31–35]. From the diagram, copper is found to extend the β -zirconium region and so acts as a β -zirconium stabilizer. In the present study, the optical microstructural observation of Zr–Cu binary specimens showed no distinguishable changes in the final heat-treated microstructures (α annealed) with increasing copper content from 0.1 to 0.8 wt%. Any trace of β -phase was not observed in any of the specimens. The reason for this may be that the β -phase was entirely transformed to α -phase during the β -quenching step or that any β -phase left over from the β -quenching was transformed to the α -phase during the following α annealing. In this work, the β -quenched structure with copper contents was not investigated. However, copper addition in the present study does not seem to affect the final α annealed microstructure.

Table 2

Size and area fraction of precipitates in the modified Zry-4 alloys

Specimen number	Particle size (μm)			Area fraction (%)
	Average	Min.	Max.	
1	0.10	0.04	0.25	1.13
2	0.13	0.05	0.53	2.23
3	0.16	0.03	0.57	3.92
4	0.12	0.03	0.47	1.94
5	0.13	0.03	0.48	2.33
6	0.16	0.03	0.51	2.88
7	0.11	NA ^a	0.68	3.23
8	0.18	NA	0.53	3.77
9	0.22	NA	0.62	4.63
10	0.25	NA	0.69	4.77
11	0.29	NA	0.72	8.61
12	0.12	0.04	0.35	2.12

^a Not analyzed.

It is well known that the small grain size of the metal matrix increases the oxygen diffusion rate resulting in an increase in the oxidation rate. In the present study, the grain size in the Zr–Cu binary alloys drastically decreased as the copper content increased from 0 to 0.3 wt%. It was considered that grain growth was suppressed due to the grain boundary pinning effect of Zr_2Cu precipitates. However, in case of copper-added modified Zry-4 alloys, the copper addition did not significantly change the grain size. It is probable that the same grain size is obtained because the pinning effect of Zr_2Cu precipitates is much less effective than that of $Zr(Cr, Fe)_2$ precipitates; in the copper-added modified Zry-4 alloy, $Zr(Cr, Fe)_2$ precipitates were also present as well as Zr_2Cu precipitates and the number of $Zr(Cr, Fe)_2$ precipitates were much larger than that of Zr_2Cu precipitates.

4. Summary

In the present study, the effects of copper on the oxidation behavior were studied. The purpose of the work is not to present an oxidation model that may describe the oxidation performance of the modified Zry-4 in a general manner. Rather, our intent is to determine whether a copper addition to zirconium alloys can affect the oxidation behavior, and to find the optimum copper content for the improved oxidation properties of cladding materials. The work has been carried out as a preliminary study. The weight gains measured are based on short-term experiments. In many cases, the long-term characteristic of weight gain follows the tendency of the short-term characteristic. However, the long-term behavior like weight gain in the post-transition region can be different from short-term characteristics. Thus, it is necessary to verify the oxidation characteristics of the modified Zry-4 alloys in the long-term experiment.

In autoclave tests for 100 days exposure at 360°C, the measurement of weight gain in the modified Zry-4 alloys showed that small additions of copper lowered the weight gain while further additions of more than about 0.2 wt% increased the weight gains. So, the optimum copper concentration for improved oxidation resistance is thought to be around 0.1–0.2 wt%. In this work, the weight gains of the candidate alloys were lower by 30% than that of Zry-4. Moreover, as to the mechanical properties, the ultimate tensile strength was nearly equal to that of Zry-4 [5]. Thus, it is considered that copper is one of the candidate alloying elements for improved cladding materials like niobium.

It is to be noted that numerous precipitates less than 30 nm were observed in the TEM study. However, these precipitates were excluded in calculations of the area fraction and the average size of precipitates due to the difficulty in observation. It is probable that these small

precipitates less than 30 nm were important for oxidation and mechanical properties in zirconium alloys. It is to be noted that weight gain data are compared with the characteristics of some oxidation processes in the present study, but no dominant rate-determining process has been found.

Acknowledgements

This study was supported by Korea Electric Power Corporation (KEPCO) and Electrical Engineering and Science Research Institute (EESRI) and by the Brain Korea 21 project.

References

- [1] H.S. Hong, S.J. Kim, K.S. Lee, *J. Nucl. Mater.* 238 (1996) 211.
- [2] H.S. Hong, S.J. Kim, K.S. Lee, *J. Nucl. Mater.* 273 (1999) 177.
- [3] D. Charquet, J.P. Gros, J.F. Wadier, in: *International Topic Meeting on LWR Fuel Performance*, Avignon, France, April 21–24, 1991, p. 143.
- [4] F. Garzarolli, R. Schumann, E. Seinberg, in: *Proceedings of the 10th International Symposium on Zirconium in the Nuclear Industry*, ASTM STP, vol. 1245, 1993, p. 709.
- [5] H.S. Hong, H.S. Kim, S.J. Kim, K.S. Lee, *J. Nucl. Mater.* 280 (2000) 230.
- [6] P. Rudling, G. Wikmark, *J. Nucl. Mater.* 265 (1999) 44.
- [7] H. Anada, K. Takeda, S. Hagi, in: *International Topic Meeting on LWR Fuel Performance*, Park City, UT, April 10–13, 2000, p. 445.
- [8] ASTM G-2, *Standard Test Method for Corrosion Testing of Products of Zirconium, Hafnium, and Their Alloys in Water at 680°F or in Steam at 750°F*, 1993, p. 47.
- [9] D.R. Clark, F. Adar, *J. Am. Ceram. Soc.* 65 (1982) 284.
- [10] R.C. Gavie, P.S. Nicholson, *J. Am. Ceram. Soc.* 55 (1972) 303.
- [11] V.G. Keramidis, W.B. White, *J. Am. Ceram. Soc.* 57 (1974) 22.
- [12] M.G. Fontana, *Corrosion Engineering*, McGraw-Hill, New York, 1986, p. 513.
- [13] H.A. Porte, *J. Electrochem. Soc.* 107 (1960) 506.
- [14] T. Isobe, Y. Matsuo, in: *Proceedings of the 9th International Symposium on Zirconium in the Nuclear Industry*, ASTM STP, vol. 1132, 1991, p. 346.
- [15] F. Garzarolli, H. Sedel, R. Tricot, J.P. Gros, in: *Proceedings of the 9th International Symposium Zirconium in the Nuclear Industry*, ASTM STP, vol. 1132, 1991, p. 395.
- [16] B. Cox, in: *Proceedings State Committee Utilisation Atomic Energy of the USSR Conference on Reactor Materials Science*, Alushta, USSR, 1978.
- [17] N. Ramasubramanian, *J. Electrochem. Soc.* 127 (1980) 2566.
- [18] H. Stehle, F. Garzarolli, A. Garde, P. Smerd, ASTM STP, vol. 824, 1984, p. 483.

- [19] J. Godlewsky, in: Proceedings of the 10th International Symposium on Zirconium in the Nuclear Industry, ASTM STP, vol. 1145, 1994, p. 663.
- [20] P. Aldebert, J. Traverse, *J. Am. Ceram. Soc.* 68 (1985) 34.
- [21] M. Harada, M. Kimpara, K. Abe, in: Proceedings of the 9th International Symposium on Zirconium in the Nuclear Industry, ASTM STP, vol. 1132, 1991, p. 368.
- [22] R. Kuwae, K. Sato, E. Higashinakawada, K. Kawashima, S. Nakamura, *J. Nucl. Mater.* 119 (1983) 229.
- [23] S. Abolhassani, D. Gavillet, F. Groeschel, P. Jourdain, H.U. Zwicky, in: International Topic Meeting on LWR Fuel Performance, Park City, UT, April 10–13, 2000, p. 470.
- [24] G. Lelievre, C. Tessier, X. Iltis, B. Berthier, F. Lefebvre, *J. Alloys Comp.* 268 (1998) 308.
- [25] O. Canet, M. Latroche, F. Boureevigneron, A. Percheronguegan, *J. Alloys Comp.* 210 (1994) 129.
- [26] T. Kubo, Y. Wakashima, H. Imahashi, M. Nagai, *J. Nucl. Mater.* 132 (1985) 126.
- [27] Y. Hatano, M. Sugisaki, *J. Nucl. Sci. Technol.* 34 (3) (1997) 264.
- [28] H.S. Hong, S.J. Kim, K.S. Lee, *J. Nucl. Mater.* 265 (1999) 108.
- [29] S. Banerjee, R. Krishnan, *Metall. Trans.* 4 (1973) 1811.
- [30] L. Wadekar, V.V. Raman, S. Banerjee, M.K. Asundi, *J. Nucl. Mater.* 151 (1988) 162.
- [31] C.E. Lundin, D.J. McPherson, M. Hanson, *Trans. AIME* 197 (1953) 273.
- [32] T.B. Massalski, *Binary Alloy Phase Diagrams*, 2nd Ed., ASM, 1990, p. 1511.
- [33] D.L. Douglass, R.E. Morgan, *Trans. AIME* 215 (1959) 869.
- [34] L. Bsenko, *J. Less-Common Met.* 40 (1975) 365.
- [35] R.P. Elliott, *Constitution of Binary Alloys*, McGraw-Hill, New York, 1965.